ELSEVIER

Colloids and Surfaces A: Physicochem. Eng. Aspects 255 (2005) 73–78

COLLOIDS AND SURFACES A

www.elsevier.com/locate/colsurfa

Self-aggregation in dimeric arginine-based cationic surfactants solutions

Daphne Weihs[a,1], Dganit Danino[a,2], Aurora Pinazo-Gassol[b], Lourdes Perez[b], Elias I. Franses[c], Yeshayahu Talmon[a,*]

[a] *Department of Chemical Engineering, Technion—Israel Institute of Technology, Haifa 32000, Israel*
[b] *Department of Surfactant Technology, IIQAB-CSIC, J. Girona 18-26, 08034 Barcelona, Spain*
[c] *School of Chemical Engineering, Purdue University, 480 Stadium Mall Drive, West Lafayette, IN 47907-2100, USA*

Received 28 August 2004; accepted 26 November 2004
Available online 13 January 2005

Abstract

We investigated the microstructures formed in aqueous solutions of the cationic amino acid-based monomeric, methyl ester of N^{α}-lauroyl arginine (LAM) and its dimeric molecules ($C_n(LA)_2$), and examined the effect of a perturbation of the local arrangement of polar heads, by the spacer length, on the micellar and mesomorphic properties of surfactants in aqueous solutions.

We employed cryogenic-temperature-transmission electron microscopy (cryo-TEM) to image microstructures appearing as a function of spacer length and concentration. The microstructures observed in the monomeric LAM solutions were consistent with those of a single-tailed surfactant with a large head-group. Our results show that the dimeric arginine-based surfactants tend to form aggregates of lower curvature than the corresponding monomeric surfactants. In the short spacer (3-carbon) dimeric molecule the microstructures observed were spheroidal micelles that changed to thread-like micelles and disk-like structures as the concentration was increased. The dimeric molecules with longer spacers exhibited lower-curvature microstructures, mainly flat and twisted-ribbons. Those microstructures appeared at lower concentrations as the spacer became longer and more hydrophobic. When the spacer no longer inhibits head-group separation ($n > 3$), low curvature, twisted-ribbons are the preferred structure of this system. In all likelihood, ribbons form because of chirality of the amphiphiles, and enhanced hydrogen bonding of the spacer with the surrounding water that leads to rigid filament-like structures.

Keywords: Dimeric surfactants; Arginine; Cryo-TEM

1. Introduction

Dimeric or gemini surfactants [1,2] are composed of two identical or different amphiphilic moieties joined together at or near the head-groups by a spacer group. Linking the surfactants this way, provides an additional parameter to control self-aggregation and some of the surfactant properties [3]. The spacer is usually chosen to be a simple alkane chain [2]. Other spacers, such as alkenes with an amide or disulfide bond [4–6], or phenylenedimethylene groups [7] have also been used. Dimeric surfactants have been shown to be superior to conventional, monomeric surfactants. They have a much lower critical micelle concentration (CMC) and effective surfactant and antimicrobial behavior [3]. In general, they are more effective in adsorbing at the aqueous solution/air interface, reducing the surface tension, and forming micelles at lower concentrations [8,9].

Zana and Talmon [2] showed that a short alkane chain spacer (usually about 2–3 carbons long) imposes reduced

* Corresponding author. Tel.: +972 4 8292007; fax: +972 4 8295672.
E-mail address: ishi@tx.technion.ac.il (Y. Talmon).
[1] Present address: Department of Pathology and Chemistry, David Geffen School of Medicine, UCLA, Los Angeles, CA 90095, USA.
[2] Present address: Department of Biotechnology and Food Engineering, Technion—Israel Institute of Technology, Haifa 32000, Israel.

0927-7757/$ – see front matter © 2004 Elsevier B.V. All rights reserved.
doi:10.1016/j.colsurfa.2004.11.035

intermonomeric head-group separation. The short spacer is probably fully stretched at the water-core interface [10]. This influences the distribution of distances between the polar heads at the interface, the spontaneous curvature of the surfactant layer, and, in turn, the shape of the aggregates formed by those surfactants. With larger, more hydrophobic spacers progressive penetration of the spacer into the aggregate core is also expected, as the spacer becomes flexible enough and too hydrophobic to remain in the aqueous phase.

Dimeric surfactants, of two-alkyl di-methyl quaternary ammonium groups linked by a hydrocarbon spacer chain at the head-groups level, have been studied extensively [10,11]. Those surfactants have excellent properties of solubilization, soil cleanup, and oil recovery [3]. However, quaternary ammonium salts are very stable molecules with poor chemical and biological degradability [5].

Infante et al. [12] studied arginine-based lipoaminoacid surfactants and their dimeric counterparts [5]. These surfactants' high biocompatibility, antimicrobial and surfactancy properties, relative to conventional surfactants, make them interesting for application in many fields, such as cosmetic, food, and pharmaceutical technologies [13]. The monomeric molecule exhibited classical single CMC behavior followed by an isotropic region to about 22 wt.% [5] and above that a hexagonal liquid crystalline phase was observed by light microscopy. Unlike the monomer, the related gemini surfactants showed non-classical behavior of two apparent CMCs. The first CMC, at which the equilibrium surface tension behavior shows a classical "break", to a value unchanged with increasing concentration, is about 1000–3000 times smaller than the CMC of the monomer [8]. However, measurements by conductivity, counterion thermodynamic activity, and solubilization/fluorescence behavior show a break, or second CMC, at a concentration of about 80–200 times the first CMC, or about 20 times less than the CMC of LAM [9]. The solubilities of $C_n(LA)_2$ in water at 25 °C depend on the spacer chain length. $C_3(LA)_2$ formed an isotropic liquid single phase up to 9%, $C_6(LA)_2$ up to 4%, and $C_9(LA)_2$ up to 0.8% [5].

In this work, we investigated the microstructures formed in aqueous solutions of monomeric and dimeric arginine-based surfactants as a function of spacer length and concentration.

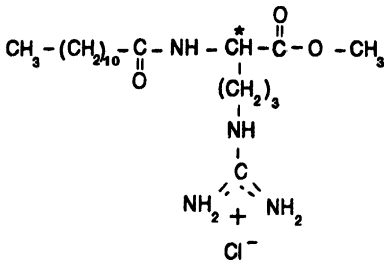

Scheme 1. Molecular structure of the single chain surfactant LAM. (*) Indicates a chiral center.

2. Materials and methods

2.1. Materials

Cationic amino acid-based monomeric, methyl ester of N^{α}-lauroyl arginine (LAM) (Scheme 1), and dimeric, N^{α},N^{ω}-bis (N^{α}-acylarginine) α,ω-dialkyl-amides (Scheme 2), surfactants were synthesized at the Department of Surfactant Technology, IIQAB-CSIC, Spain, as described elsewhere [5,12]. Dimeric surfactants with 3, 6, 9 and 12 carbon atoms in the spacer were examined (Scheme 2), and will be referred to as $C_n(LA)_2$, n = spacer carbon atoms from here on.

2.2. Sample preparation

Powder-samples were dissolved in Millipore Milli-Q water to concentrations above the CMC [5,13], and left at room temperature for 2 days to equilibrate. Solutions were in general clear, isotropic, and low viscosity. At the high LAM and $C_{12}(LA)_2$ concentrations, however, solutions were not clear anymore and their viscosity increased. Concentrations were chosen so as to be above the CMC but still in the isotropic region.

2.3. Cryogenic-temperature-transmission electron microscopy (cryo-TEM)

Samples for cryo-TEM were prepared by vitrification in a controlled environment vitrification system (CEVS) at 25 °C and 100% relative humidity. The CEVS apparatus is described in detail elsewhere [14]. A drop of the solution was placed on a perforated carbon film, supported on an elec-

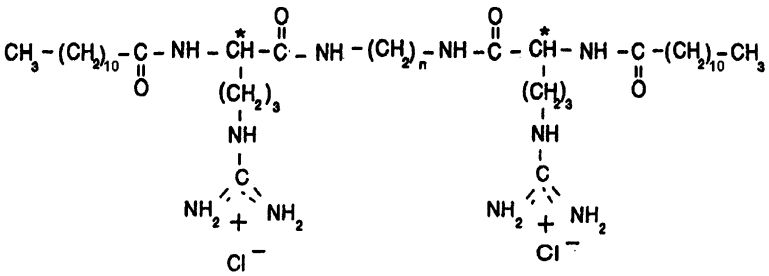

Scheme 2. Molecular structure of N^{α},N^{ω}-bis (N^{α}-acylarginine) α,ω-dialkyl-amides or $C_n(LA)_2$.

tron microscope copper grid, held by tweezers in the CEVS. The drop was then blotted with filter paper to a thickness of 20–300 nm and the resulting thin film was immediately plunged into liquid ethane at its freezing point (−183 °C) causing its vitrification. The vitrified specimen was then stored under liquid nitrogen (−196 °C), and later transferred into a Philips CM120 microscope, operated at 120 kV, in an Oxford CT-3500 cold-stage system. Images were taken in the low-dose imaging mode, to minimize electron-beam radiation damage, and at a nominal underfocus of 3–5 μm, to enhance mass-thickness contrast by phase contrast. Images were recorded digitally by a Gatan 791 MultiScan CCD camera, using the Digital Micrograph 3.1 software package.

3. Results

The monomer, LAM, was examined following the previously determined phase diagram [13]. LAM exhibited classical single CMC behavior followed by an isotropic region to about 22 wt.% [5]. Concentrations were chosen above the CMC [8] where the solution exhibited isotropic behavior. Typical microstructures for this system are shown in Fig. 1. At concentrations up to 7.5 wt.% only spheroidal micelles, 3–5 nm in diameter, were imaged (Fig. 1A and B), as may be expected for a surfactant with a large head-group and single hydrocarbon chain [15]. A further increase in concentration to 9 wt.% produced ordered, rippled structures (Fig. 1C), their short dimension about 5 nm. Those structures spanned the entire grid, did not seem affected by flow produced in sample preparation [16], and may be bundles of threadlike micelles, or possibly disordered hexagonal phase, projected perpendicularly to the long axes of the micelles. No spheroidal micelles were visualized in the background. The ordered phase became more densely packed and ordered as the concentration was raised further. The appearance of the 18 wt.% solution (Fig. 1D) was reminiscent of the two-dimensional hexagonal liquid crystal phase seen in diblock copolymers after annealing [17], including a “grain boundary”, marked by arrows.

In the gemini surfactant homologue with the 3-carbon ($n = 3$) spacer ($C_3(LA)_2$) the dominant microstructures at the lowest concentrations, 1.3 wt.%, were spheroidal micelles (Fig. 2A). Few twisted-ribbon-like structures were also seen, as in Fig. 2B. Those twisted-ribbons appear to change electron density along their length. Darker streaks (arrowheads in Fig. 2B) appear when the ribbon segment is imaged side-on by the electron beam. In areas, where the ribbon is imaged face-on, the contrast between the ribbon and the vitrified water matrix is low, and the ribbons appear to be almost transparent (arrows in Fig. 2B).

As the concentration was increased (4 wt.%), flexible thread-like micelles, with some branching, appeared and coexisted with a few spheroidal micelles (Fig. 2C). Some disk-like structures were also visualized, as shown in Fig. 2D. With further concentration increase to the upper limit of the

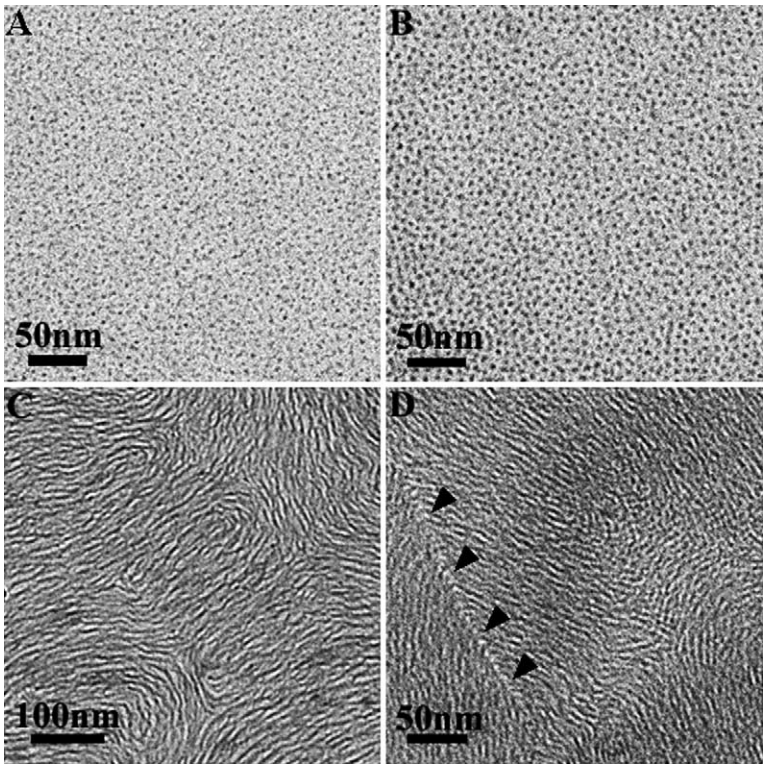

Fig. 1. Electron micrographs of vitrified LAM solutions (A) spheroidal micelles at 4.3 wt.%; (B) spheroidal micelles at 7.5 wt.%; (C) densely packed, elongated, rippled structures at 9 wt.%; (D) dense ordered phase at 18 wt.%; arrowheads mark a “grain boundary” between ordered domains.

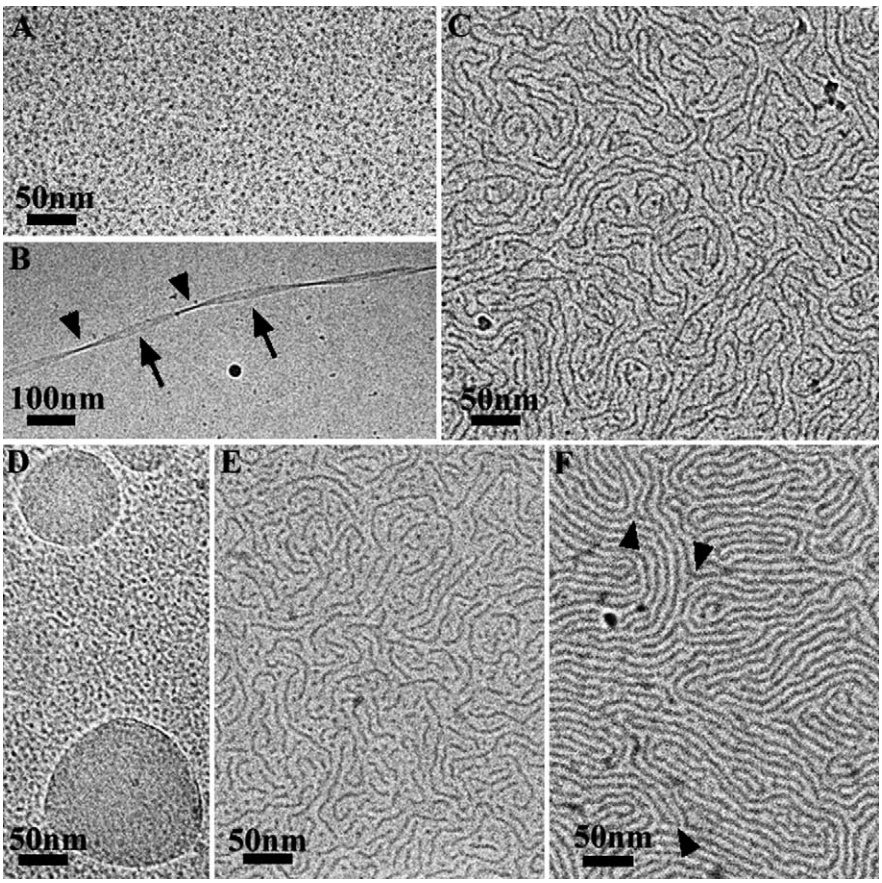

Fig. 2. Electron micrographs of $C_3(LA)_2$: (A) spheroidal micelles at 1.3 wt.%; (B) single twisted-ribbon at 1.3 wt.%; arrows mark regions where the ribbon lays flat on the grid and arrowheads mark regions where the ribbon twists; (C) long thread-like micelles at 4 wt.%. Dark spots are small ice crystals that do not affect the microstructures; (D) disk-like structures and spheroidal micelles at 4 wt.%; (E) short thread-like micelles and spheroidal micelles at 8 wt.%; and (F) tightly packed, long, branched thread-like micelles at 8 wt.% arrows mark branching points.

isotropic region (8 wt.%, as determined by light microscopy) short, flexible thread-like micelles were the main structure (Fig. 2E). However, long, sometimes branched-thread-like micelles were also visualized in some regions (Fig. 2F, arrowheads mark branching points). Those variations may be due to changes in local concentration on the grid. Those thread-like micelles were short (up to 200 nm), relative to some seen at 4 wt.%. Spheroidal micelles were still present, but their number density was significantly reduced, and no disk-like structures were observed.

The intermediate length homologue with the 6-carbon spacer ($C_6(LA)_2$) exhibited spheroidal micelles coexisting with twisted-ribbon structures and some disk-like structures throughout the concentration range identified previously as the isotropic region [5]. The twisted-ribbon structures in this homologue seemed to group together in locally thicker areas of the vitrified specimen (Fig. 3A), while in other, thinner areas only spheroidal micelles were observed (not shown).

The 9-carbon spacer homologue ($C_9(LA)_2$) exhibited flat-ribbons, some twisted. At a low concentration solution (0.1 wt.%), the ribbons appeared to be twisted (Fig. 3B), and few had periodic twists (as in Fig. 2B). When the concentration was increased to 0.7 wt.% few ribbons were tightly twisted and most exhibited what appeared to be either a partial twist, or pinch in the bilayer (arrows in Fig. 3C). Those darker lines are connected by a membrane (the ribbon structure) and are not simply two aligned thread-like micelles. In some cases, this pinch in the ribbons showed signs of a twist as in the inset in Fig. 3C. Those pinched-ribbons may be part of a process of twist unfolding or an incomplete twist. They may be intermediate structures forming before the isotropic to hexagonal phase transition that was observed by Perez et al. [5] at about 0.8 wt.%. Many thin, rod-like structures, 6–8 nm in diameter, were also seen in the higher concentration (arrowheads in Fig. 3C). Those structures may have been straightened and aligned because of the flow during sample preparation. No spheroidal micelles were seen in the background in any of the $C_9(LA)_2$ concentrations examined.

In the homologue with the longest spacer ($n = 12$), the only observed microstructures were ribbons (Fig. 3D). In this homologue, no spheroidal micelles were seen in the background at the concentrations examined. Most of the ribbons visualized were twisted, but some seemed rather short, stiff, and flat.

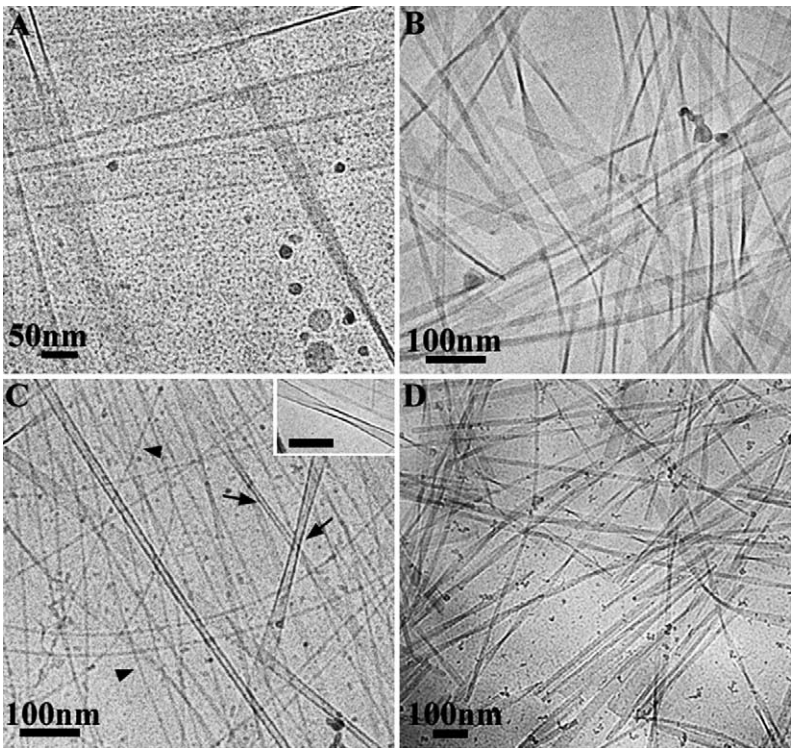

Fig. 3. Electron micrographs of long spacer dimeric surfactants (A) twisted-ribbons, spheroidal micelles, and small disk-like structures in $C_6(LA)_2$ at 1.3 wt.%; (B) twisted-ribbons in $C_9(LA)_2$ at 0.1 wt.%; (C) partially twisted ("pinched")-ribbons (arrows), and thread-like ribbons or fibers (arrowheads) in $C_9(LA)_2$ at 0.7 wt.%; Inset shows a twisted-pinched-ribbon (bar 50 nm); (D) twisted- and flat-ribbons in $C_{12}(LA)_2$ at 0.05 wt.%.

4. Discussion

We have examined the microstructures appearing in LAM and its dimeric derivatives. LAM solutions showed structures typical of a single-tailed surfactant with a large head-group. Solans et al. [18] showed by light microscopy of LAM, that the favored structure after exceeding the solubility limit of micelles in water (i.e., about 20 wt.% at 25 °C [13]) is that of a hexagonal liquid crystal. Based on that information, they assumed that at high surfactant concentrations, close to the phase transition, LAM would assemble into cylindrical micelles. We observed that, as the concentration is increased and approaches the phase-transition concentration, elongated structures in an ordered array appear. Those structures may be tightly packed thread-like micelles in a hexagonal array. However, it is not possible to determine that conclusively from the cryo-TEM data, because no cross-sections showing a hexagonal array were observed, since elongated structures tend to be present in the specimen with their long dimension perpendicular to the beam.

The dimeric homologues, with spacers of 6, 9, and 12, carbons all showed similar structures, i.e., twisted-ribbons. However, the homologue with the shortest spacer (3-carbon) exhibited structures more similar to those seen in the LAM. Experimental [2,10] and theoretical [19,20] studies have indicated that a short spacer imposes reduced head-group separation, thus affecting the shapes of the formed microstructures. Accordingly, for the case of the short (3-carbon) spacer few ribbon-like, bilayer structures are seen and a transition from spheroidal micelles to entangled, thread-like micelles is seen at relatively low concentrations, with intermediate disk-like microstructures. This effect is inverse to the one observed in another dimeric surfactant system [10].

In the transition from spheroidal to thread-like micelles (at 4 wt.%), we notice the absence of short and medium length cylindrical micelles, with length of several times the diameter of a spheroidal micelle. Similar behavior has been reported for another cationic gemini surfactant [21] and has been attributed to the unfavorable high energy of the intermediate length structures [22].

It has been reported that longer spacers progressively penetrate into the aggregate core, as the spacer becomes flexible enough and too hydrophobic to remain in the aqueous phase [2]. This increases the volume of the hydrophobic segment of the molecule and lowers the curvature of the microstructures formed. In this study, we observed that as the spacer became longer and more hydrophobic, the twisted-ribbon structures appeared at lower concentrations and replaced the spheroidal micelles altogether.

Twisted-ribbon structures are a characteristic feature of this system. We hypothesize that they occur because of the double-chirality of the gemini molecule (Scheme 2) and the spacer composition. Oda et al. [23] found that adding chiral counter-ions to a gemini surfactant produces twisted-ribbons, similar to those seen here. They suggested that the presence of the highly anisotropic-ribbon structures im-

plies long-range alignment of the constituent molecules that may be correlated with a hydrogen-bonded network of the counter-ions. Introduction of secondary amide bonds into the head-groups (i.e., in the spacer), as in the dimeric surfactant examined here, leads to strong hydrogen bonding within the molecule and to surrounding water and other gemini molecules, that in turn leads to more rigid, filament-like microstructures [24].

In summary, the microstructures observed in the monomeric LAM are consistent with those of a single-tailed surfactant with a large head-group, while the dimeric arginine-based surfactants tend to form aggregates of lower curvature than the corresponding monomeric surfactants.

Acknowledgement

We thank Mrs. B. Shdemati for her assistance in the sample preparation. The TEM work was performed at the Hannah and George Laboratory for advanced electron microscopy.

References

[1] F.M. Menger, C.A. Littau, J. Am. Chem. Soc. 113 (1991) 1451.
[2] R. Zana, Y. Talmon, Nature 362 (1993) 228.
[3] R. Zana, in: K. Holmberg (Ed.), Novel Surfactants: Preparation, Applications, and Biodegradability,, Marcel Dekker, New York, 1998, p. 241.
[4] M. Diz, A. Manresa, A. Pinazo, P. Erra, M.R. Infante, J. Chem. Soc. Perkin Trans. 2 (1994) 1871.
[5] L. Perez, J.L. Torres, A. Manresa, C. Solans, M.R. Infante, Langmuir 12 (1996) 5296.
[6] A. Pinazo, M. Diz, C. Solans, M.A. Pes, P. Erra, M.R. Infante, J. Am. Oil Chem. Soc. 70 (1993) 37.
[7] N. Hattori, A. Yoshino, H. Okabayashi, C.J. O'Connor, J. Phys. Chem. B 102 (1998) 8965.
[8] L. Perez, A. Pinazo, M.J. Rosen, M.R. Infante, Langmuir 14 (1998) 2307.
[9] A. Pinazo, X. Wen, L. Perez, M.R. Infante, E.I. Franses, Langmuir 15 (1999) 3134.
[10] D. Danino, Y. Talmon, R. Zana, Langmuir 11 (1995) 1448.
[11] R. Zana, M. Benrraou, R. Rueff, Langmuir 7 (1991) 1072.
[12] M.R. Infante, J.G. Dominguez, P. Erra, R. Julia, M. Prats, Int. J. Cosmet. Sci. 6 (1984) 275.
[13] C. Solans, M. Infante, N. Azemar, T. Warnheim, Progr. Colloid Polym. Sci. 79 (1989) 70.
[14] J.R. Bellare, H.T. Davis, L.E. Scriven, Y. Talmon, J. Electron Microsc. Technol. 10 (1988) 87.
[15] C. Tanford, The Hydrophobic Effect: Formation of Micelles and Biological Membranes, second ed., John Wiley and Sons, New York, 1980 (Chapter 2).
[16] Y. Zheng, Z. Lin, J.L. Zakin, Y. Talmon, H.T. Davis, L.E. Scriven, J. Phys. Chem. B 104 (2000) 5263.
[17] S. Förester, A.K. Khandpur, J. Zhao, F.S. Bates, I.W. Hamley, A.J. Ryan, W. Bras, Macromolecules 27 (1994) 6922.
[18] C. Solans, M.A. Pés, N. Azemar, M.A. Infante, Progr. Colloid Polym. Sci. 81 (1990) 144.
[19] H. Diamant, D. Andelman, Langmuir 10 (1994) 2910.
[20] T.A. Camesano, R. Nagarajan, Colloids Surf. 167 (2000) 165.
[21] A. Bernheim-Groswasser, R. Zana, Y. Talmon, J. Phys. Chem. B 104 (2000) 4005.
[22] S. May, A. Ben-Shaul, J. Phys. Chem. B 105 (2001) 630.
[23] R. Oda, I. Huc, M. Schmutz, S.J. Candau, F.C. MacKintosh, Nature 399 (1999) 566.
[24] J.H. Fuhrhop, D. Spiroskit, C. Boettcher, J. Am. Chem. Soc. 115 (1993) 1600.